

# 3.5-inch High-Performance Disk Drives for Enterprise Applications: AL-7 Series

●Keiji Aruga

*(Manuscript received September 25, 2001)*

**Fujitsu offers the new AL-7 series of high-performance SCSI drives for server applications. The series consists of a 73G-byte, 10 000 rpm model and a 36G-byte, 15 000 rpm model. This paper describes how the mechanisms of these drives were improved to reduce their power consumption and make them fast, highly reliable, and acoustically quiet. We describe how the non-repeatable run-out (NRRO) was reduced by stabilizing the internal airflow and reducing resonance in the spindle motor. Next, we describe the new lightweight, rigid actuator and servomechanisms we developed to increase the access speed and the steps that were taken to reduce the drives' acoustic noise and increase their reliability. Finally, we present the results of some benchmark tests we conducted on these drives.**

## 1. Introduction

The rapid popularization of the Broadband Internet is creating a demand for larger and faster servers. Since a server's main function is to store data, storage systems must be based on fast, high-capacity storage devices. Especially, the broadband system needs a wider bandwidth in terms of storage, transfer rate, and random access performance. Recently, RAID systems, the overall performance of which is proportional to the drive performance, are being used as enterprise servers. In low-end servers, some trial ATA RAID5s are being prompted; however, larger and more reliable systems cannot be achieved without higher rotational speed SCSI drives.

Fujitsu is now offering the new-generation AL-7 series of high-performance SCSI hard disk drives for server applications. Since the first shipment of Eagle drives in 1981, Fujitsu has been a pioneer of high-end drives for many OEM customers.<sup>1)</sup> In 1993, the first 3.5-inch AL-1 equipped

with MR heads was introduced. After the shipment of the AL-4 in 1997, the new generation of drives was widely used by many OEM customers because of their high reliability. With the AL-5s, we introduced the world to high-performance 10 000 (10 k) rpm and smaller size 3-inch (84 mm) media in 1998.<sup>2),3)</sup>

We have now developed the AL-7 series new-generation platform. The series consists of the AL-7LE (MAN3xxx) large-capacity, 10 krpm (18 to 73 GB) drives with 3-inch media and the new AL-7LX (MAM3xxx) 15 krpm, high-end drives (18/36 GB) with 2.75-inch (70 mm) media. The AL-7LX drives are Fujitsu's first generation of 15 krpm drives. The series has both an Ultra160 SCSI and 2 Gb/s Fibre Channel interface. The AL-7 series features not only excellent IO performance, but also environment friendly features, for example, lower power requirements and lower acoustic noise.

This paper gives an overview of the new AL-7

series of hard disk drives and describes their mechanical platform. The technologies used to achieve higher track densities, faster access, and less acoustic noise are also presented.

## 2. Product outline

The AL series has made remarkable progress in terms of areal density and transfer rate (Figure 1). The areal density of this series has approximate-

ly doubled each year during the past several years, and the media transfer rate has now reached almost 100 Mbyte/s. Figure 2 also shows the progress of track density, seek time, and rotational speed. The main specifications of the AL-7 drives are shown in Table 1. These SCSI drives have the highest areal density (18 GB/platter for 3-inch media), the fastest transfer rate, the fastest seek time, and the lowest acoustic noise. The

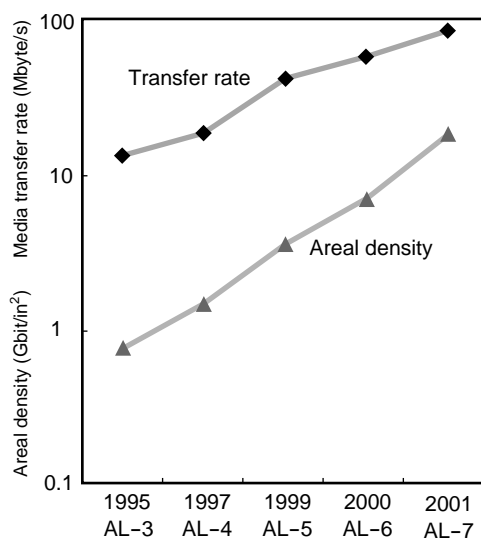


Figure 1  
Areal density and transfer rate progress.

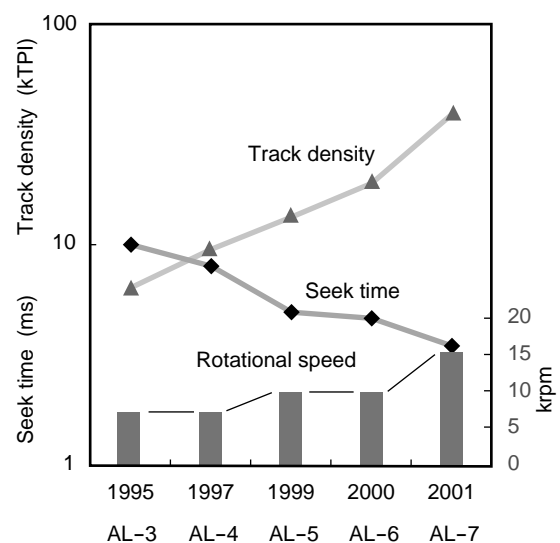


Figure 2  
Track density, seek time, and rotational speed progress.

Table 1  
Main specifications of AL-7 series.

	AL-6LE	AL-7LE	AL-7LX
Description	MAJ3364/3182/3091	MAN3735/3367/3184	MAM3367/3184
Capacity (GB)	36.4/18.2/9.1	73.5/36.7/18.4	36.7/18.4
Rotational speed (rpm)	10 025	10 025	15 000
Disk diameter (mm)	84	84	70
Disks	5/3/2	4/2/1	4/2
Heads	10/5/3	8/4/2	8/4
Media transfer rate (max.) (MB/s)	62.4	84.1	91.8
Areal density (Gbit/in <sup>2</sup> )	7.22	19.16	15.75
Bit density (BPI)	380 000	485 000	450 000
Track density (TPI)	19 000	39 500	35 000
Seek time (average) (ms)	4.7 <sup>R</sup> /5.2 <sup>W</sup>	4.5 <sup>R</sup> /5.0 <sup>W</sup>	3.5 <sup>R</sup> /4.0 <sup>W</sup>
Acoustic noise (ready) (Bels)	3.9	3.9/3.6/3.6	3.9
Power (ready) (W)	12.5/10.5/9.5	9/8/7.5	11/10
Buffer size (kbyte)	4096	8192	8192
Interface	Ultra 160	Ultra 160/FC-AL2	Ultra 160

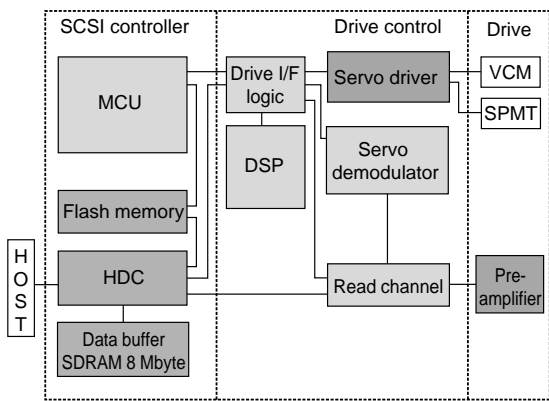


Figure 3  
Electrical block diagram.



Figure 4  
10 krpm AL-7LE (left) and 15 krpm AL-7LX (right).

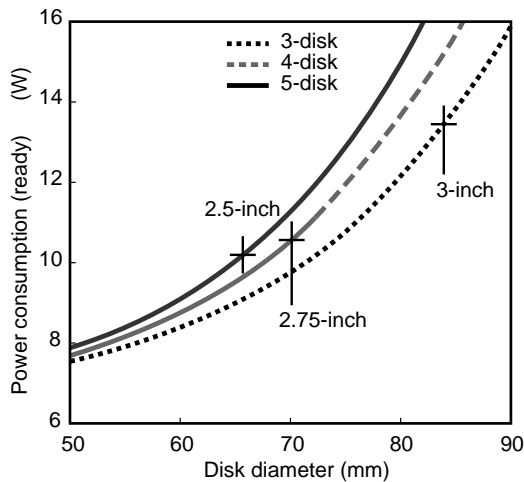


Figure 5  
Selection of disk diameter for 15 krpm.

10 krpm AL-7 drives have 2.6 times the areal density of the 10 krpm AL-6 drives, and, especially, they have twice the track density (TPI). (Usually, each generation's TPI is increased by the square root of 2, or about 40%). This high density means that fewer platters are required, which leads to a lower power consumption: for example, the AL-7LE 73 GB drive consumes less power than the AL-6LE 9 GB drive. The power consumption of the AL-7 drives has also been reduced through spindle motor optimization and improved LSI power saving control. These SCSI drives have two types of interface connectors: 68-pin and 80-pin SCA2 connectors.

The electrical architecture and chip configu-

ration, shown in **Figure 3**, are common for the AL-7LE and AL-7LX. The drive mechanisms are controlled by a high-performance ASIC, which contains a RISC microprocessor, high-performance DSP, servo demodulator, and large-capacity SRAM. The dual-processor architecture provides adequate performance to achieve a wider servo bandwidth and faster seek time. There is a large 8 M-byte interface buffer RAM to support the IO performance.

To achieve the highest areal density, a high-output Spin-filter Giant MR head and multi magnetic layered high Hc media were developed. The details of this head and media can be found elsewhere in this issue (References 4) and 5), respectively).

To make development work efficient, the 10 krpm and 15 krpm drives have a common architecture and common parts. These two types of drives have the same LSIs and printed circuit board and almost the same SCSI firmware, which is written in C++. This degree of commonality was possible because the same design team developed both drives.

**Figure 4** shows a photograph of the new AL-7LE and 7LX drives. All of the mechanisms were newly designed, and the two models use the same platform. The disk enclosure can contain up to four platters of 1 mm-thick media. This enables stiffer base casting for more precise

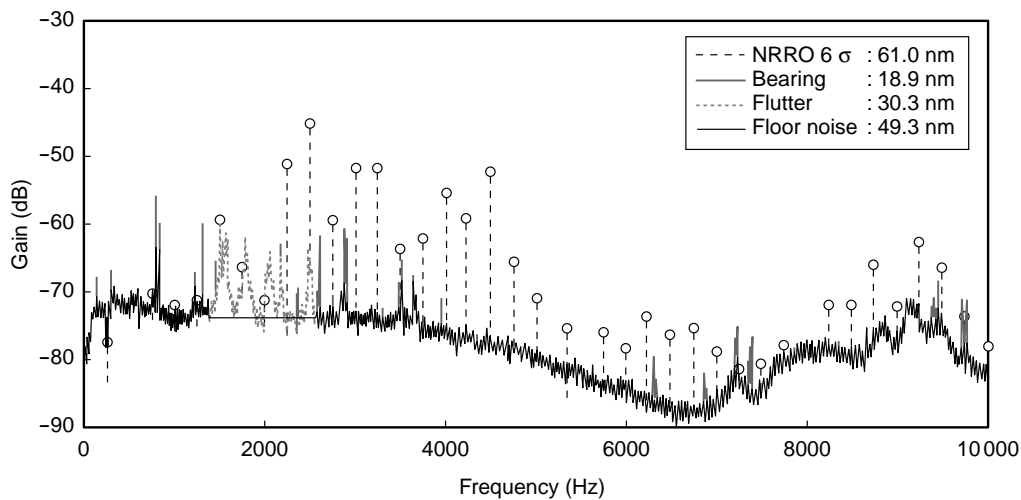


Figure 6  
NRRO spectrum of AL-7LX.

positioning, less acoustic noise, and better shock durability. To produce this platform, a new, fully automatic assembly line was developed to reduce contamination.

We will now describe our testing process. Every SCSI drive is tested for more than 100 hours. The test includes a temperature cycle running test and an input voltage change test. This strict testing ensures that each shipped drive has a very high margin of reliability.

### 3. Achieving higher TPIs at 10/15 krpm

#### 3.1 Media size selection for 15 krpm

The characteristics of higher rpm drives are largely determined by the diameters of the media. This is because the power dissipation due to disk rotation is proportional to the 4.6th power of the media diameter and the disk flutter is inversely proportional to more than the second power of the media diameter. Our design target for the 15 krpm drive was to achieve the same level of power consumption, acoustic noise, and certain other values as in the 10 krpm drive.

**Figure 5** shows an estimation of power consumption for various media diameters having the same capacity. As shown in the figure, a 3-inch (84 mm) media is out of consideration. There-

fore we had to choose either a 2.5-inch (65 mm) or 2.75-inch (70 mm) media. From the figure, we can see that the difference in power between five 2.5-inch platters and four 2.75-inch platters is less than 0.5 W. We therefore selected a 2.75-inch size as it has a good balance between power and cost. We decided on an inner diameter of 25 mm (same as in 3.5-inch media), because we could use the same spindle structure as in a 3-inch drive and because we could use the same actuator stroke as in a 2.5-inch media, which is good for the seek time.

For this selection, we estimated that the 15 krpm products will consume about the same amount of power as the 10 krpm products; that is, less than 11 W.

#### 3.2 NRRO budget

The AL-7s have about twice the track density of the AL-6s. To overcome the technical difficulties of achieving such high densities, the positioning accuracy budget was investigated in depth. The positioning error consists of the repeatable run-out (RRO) and non-repeatable run-out (NRRO). RRO is caused by the servo track writing (STW) error and motor electromagnetic excitation. NRRO is caused by electrical and mechanical disturbances. **Figure 6** shows a typical

NRRO spectrum of the position error signal. The total NRRO (which is defined by the six-sigma value) should be less than 13% of the track pitch. The AL-7LE, which has a track pitch of 0.64  $\mu\text{m}$ , requires an NRRO of 85 nm six-sigma. As the NRRO has a random distribution, we usually use the six-sigma value.

**Figure 7** shows the components of NRRO. NRRO is caused by floor noise, disk flutter, and bearing vibration. Floor noise is made up of electronic noise such as head and demodulator noise, windage disturbing the actuator at lower frequencies, windage excitation of the actuator, and head suspension at higher frequencies.

The head positioning is controlled by a closed feedback loop. The two main goals for minimizing the positioning error are to reduce the disturbance forces and increase the feedback gain.

In a higher rpm drive, the major cause of disturbance depends on the windage disturbance, which is classified into three categories. The first category is the lower frequency range (less than several hundreds of Hz). Windage excitation by airflow impinges on the actuator arm because the arm acts like a rigid body. The countermeasures to this are to reduce the windage pressure and reduce the low-frequency turbulence. The second category is disk flutter due to aerodynamic excitation,<sup>6)-8)</sup> which is located at 1.5 to 2.5 kHz in Figure 6. The third category is high-frequency vibration from the arm and suspension couple, which is caused by high-frequency turbulence.<sup>9)</sup>

These flow-related problems are now analyzed by an airflow simulation that solves the Navier-Stokes equation directly. Recent fast processors and large storages enable us to solve these problems both by a differential method or a finite element method.

**Figure 8** shows a static analysis of spoiler effects in the AL-7LE. This simulation is for lower frequency actuator disturbance. The horn-shaped spoiler rakes out the main flow to the bypass flow tunnel. Consequently, a slow airflow can be obtained between disks. The simulation predicts the velocity and pressure impinging on the arm and the windage friction loss. The measured NRRO spectrum and the increase in motor current agree well with the simulated results.

The higher frequency arm and suspension vibrations (peaks between 7 to 10 kHz in Figure 6) are explained by the unsteady flow simulation shown in **Figure 9**. This figure shows the result of solving a time-domain differential equation step-by-step.<sup>10),11)</sup> We can clearly see secondary flow Karman vortices at the wake of the arm. These vortices cause special frequency pressure

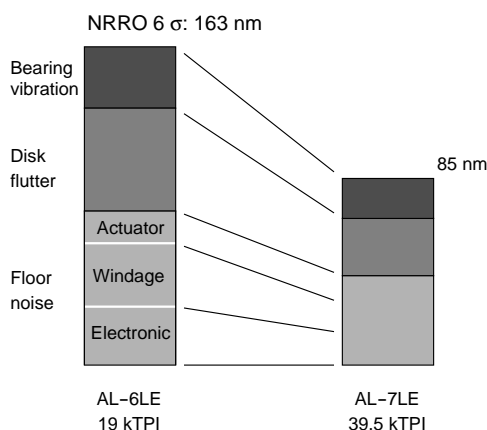


Figure 7  
NRRO budget summary.

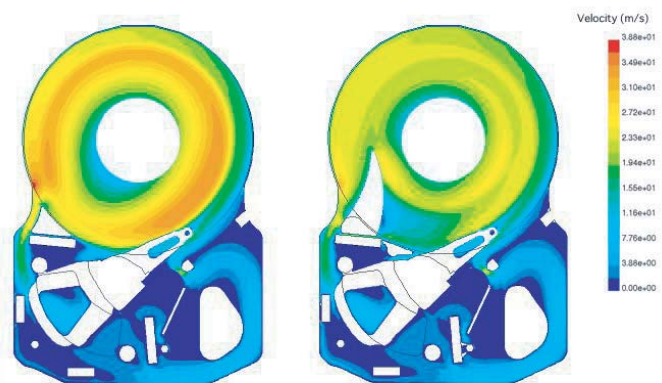


Figure 8  
Spoiler effects in airflow simulation of AL-7LE (10 krpm).

variations, usually at 5 to 10 kHz. The frequency range approximately agrees with a simple model of the Strauhl number. However, we need a huge amount of CPU time to complete the calculations. For example, the calculations needed to obtain the result shown in Figure 9 took about 1 to 2 weeks using the fastest workstation with multiple processors. We have, therefore, only reached the entrance of the true phenomena.

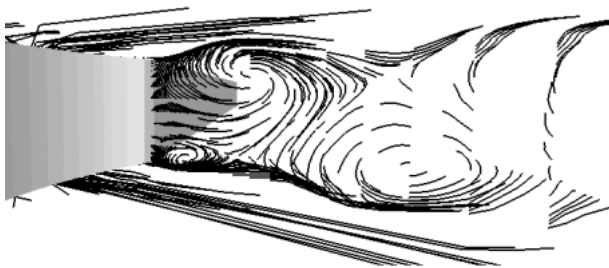
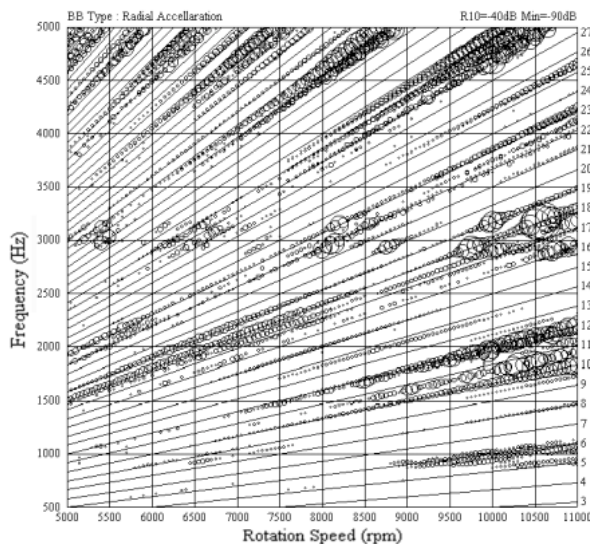


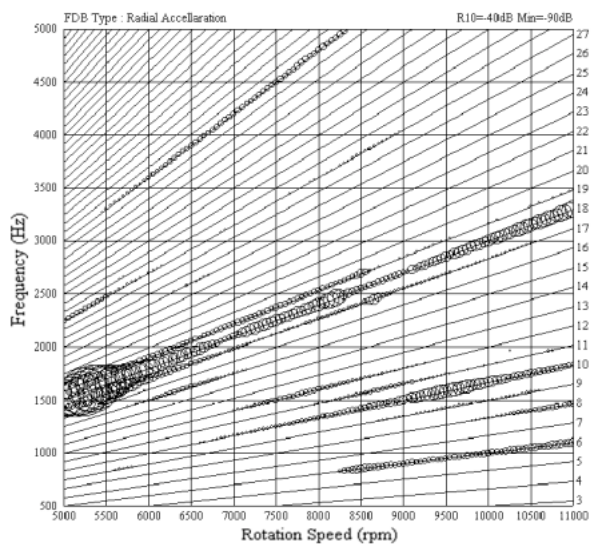
Figure 9  
Unsteady flow analysis shows Karman vortexes at the wake of the arm.

### 3.3 Solution for motor resonance problem

The next major NRRO after the one caused by the flow induced problem is due to resonances of the spindle ball bearings (these are the sharp peaks in Figure 6). If the bearing excitation frequency, which is governed by the ball and inner/outer race geometry, coincides with the spindle resonance frequency (first/second locking modes),<sup>12)</sup> we encounter considerable vibration. **Figure 10** shows a typical Campbell diagram when the spindle rotational speed is changed. In this diagram, the vibration level is indicated by each circle's diameter. The circles are centered at the point of measurement. In the figure, we can observe several regions of high resonance. To avoid these resonances, the motor design (distance between the two motor bearings, etc.) was optimized. However, because the resonance frequency is temperature dependent, it is difficult to avoid over the full operating temperature range. The most effective way we found to avoid resonances is to use a damper made of a temperature compensating material on the fixed shaft top.



(a) Ball bearing



(b) Fluid bearing

Figure 10  
Campbell diagram of AL-7LE (10 krpm).

### 3.4 Motor electromagnetic excitation<sup>13)</sup>

Once we solved the resonance problem, we focused on the electromagnetic excitation of the spindle motor. This depends on the number of poles and slots and the switching frequency of the motor. The excitation appears only at harmonics (e.g., in the case of a 3-phase, 6-pole, 9-slot motor, the major peaks are at the 6<sup>th</sup>, 10<sup>th</sup>, 12<sup>th</sup>, 18<sup>th</sup> .... harmonics). Because these excitations only occur at harmonics, we can recognize them as RROs; however, if the conditions (e.g., temperature, mounting direction) change over time, they can be treated as NRROs.

It would seem that fluid bearings could be used to avoid most of the resonance problems; however, the lower stiffness of fluid bearings sometimes enhances the electromagnetic excitation. Therefore, we need to study the electromagnetic design more thoroughly before we can use fluid bearings in our products.

### 3.5 STW improvements

Another important issue is RRO due to STW. Some portion of RRO is considered to be a frozen NRRO introduced during the STW process. The basic cause of RRO is similar to that of NRRO. However, unlike NRRO, some RRO components caused by motor excitation make the problem more complicated.

The STW used for the AL series uses an external push-pin actuator on the heavy, rigid housing. The spindle motor excitation causes a direct small disk radial motion and indirect push-pin motion. We can adjust the STW rotational speed to minimize the RRO. Usually, the lower rpm is limited by RRO degradation caused by the head flying height and the higher rpm is limited by NRRO increases on the STW. The Campbell diagram (Figure 10) clearly shows the rotational speeds at which resonance occurs. To reduce the resonance problem caused by coupling resonance between the push-pin actuator and drive actuator, a non-contact STW and an external spindle writing process are being investigated for future

products.<sup>14)</sup>

### 3.6 Fluid bearings<sup>15)</sup>

The geometrical excitation and resonance problem of ball bearings place an upper limit on the TPI of a drive. This means that we might have to implement fluid bearings in next-generation drives. The Campbell chart of a fluid bearing is shown in Figure 10 (b) with the same axes scales as in Figure 10 (a). We can see that the fluid bearing has small resonances compared with the ball bearings, but there is damped resonance starting around 1500 Hz. Heavy damping is a feature of fluid bearings, but as with ball bearings, they require measures to prevent resonance bands. As mentioned above, the excitation force of fluid bearings comes from the electromagnetic force of the motor. Refined electromagnetic design is required for the fluid bearings of higher TPI drives.

So far, we have completed the fundamental development of fluid bearing drives, and we are confident in their reliability. For server applications, however, we need to perform long-term durability and life tests before we can ship any of these drives to customers.

## 4. Fast access performance

As mentioned in Section 3, achieving a higher servo bandwidth is another important requirement for overcoming various disturbances. For example, to achieve a 40 kTPI, the bandwidth must be more than 1.4 kHz. In this section, we describe the technology we developed to achieve a high loop gain and a fast access speed in the AL-7LX 15 krpm drive.

### 4.1 Mechanical design

To achieve a higher servo bandwidth, we need an actuator with a higher mechanical resonance. **Figure 11** shows a solid model of an AL-7LX voice coil actuator. Because the seek time target is less than 3.5 ms, both a low moment of inertia and a higher resonance frequency are required. The seek time target necessitates an acceleration constant

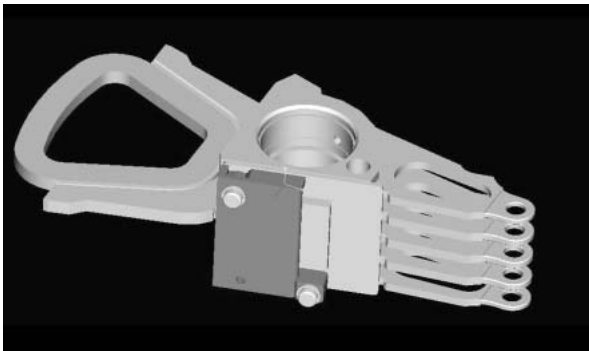


Figure 11  
High-speed actuator of AL-7LX.

of over 160 G/A (1570 m/s<sup>2</sup>/Ampere) at the rated coil resistance. To achieve this targeted high efficiency, we optimized the design of the E-block, coil, and pivot bearings. We used the highest performance permanent magnet that was available, a 50 MGOe (0.4 MJ/m<sup>3</sup>) neodymium-iron-boron magnet, in the magnetic circuit of the actuator. By optimizing the gap design, a magnetic flux density of more than 0.9 T was obtained.

By optimizing the structure and pivot bearing design, the fundamental resonance frequency was positioned at approximately 7.5 kHz, which is adequate for a servo bandwidth of 1.4 kHz.

#### 4.2 Seek performance

The high-performance actuator provides a very fast seek time. An example of the seek waveform is shown in **Figure 12**. The maximum acceleration is over 220 G (2150 m/s<sup>2</sup>). The figure shows an accurate positioning after a rapid deceleration.

The open-loop transfer function of the actuator is shown in **Figure 13**. The zero-cross frequency is 1.45 kHz with a stable phase margin of 30 degrees. The sampling frequency is 21 kHz. The fundamental resonance frequency is adequate, and a higher resonance frequency (arm and suspension) can sometimes degrade system stability. We therefore used a combined notch filter, which has several poles and zeros, to eliminate actuator resonances at higher frequencies. The

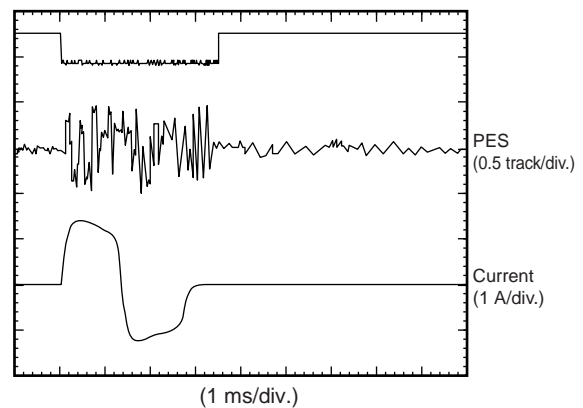


Figure12  
Seek waveform of AL-7LX (15 krpm).

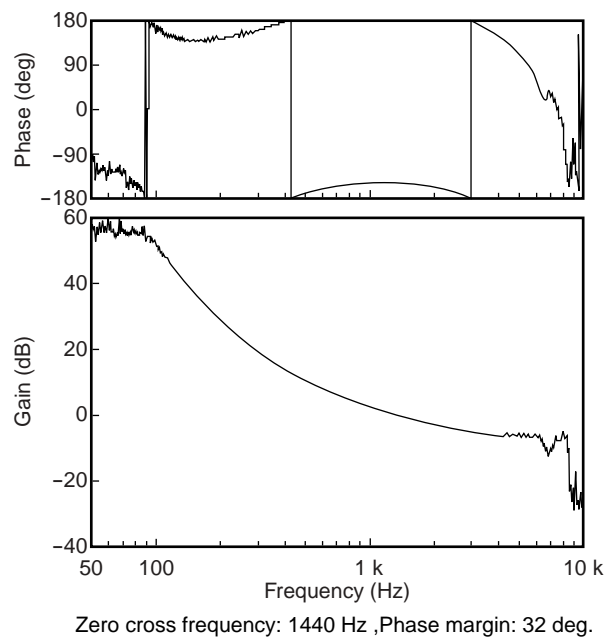


Figure 13  
Open-loop transfer function of AL-7LX (15 krpm).

filter also compensates for the temperature dependence of the actuator's resonance by using a temperature sensor attached to the drive.

#### 4.3 Servo demodulator

In this section, we describe the position demodulation of the AL series. The position error signal (PES) is demodulated by a full-phase detection system using a digital fourier transform

(DFT), and a more accurate signal is obtained by integration. The phase demodulation method is superior to the conventional amplitude demodulation scheme for decreasing the narrow track edge effect and adjacent pattern jitter effect. **Figure 14** shows an MFM (Magnetic Force Microscope) photograph of the AL-7LE. As the photograph shows, the phase shift pattern is very smooth, and as a result the PES linearity is better than that of the amplitude demodulation method.

#### 4.4 RRO compensation

In higher rpm and higher TPI drives, the low-frequency RRO caused by disk eccentricity, spindle imbalance, and thermal deformation is a very serious problem. Providing a higher servo gain is one solution (Figure 12); however, a gain of 25 dB at a rotational frequency of 250 Hz (15 000 rpm), is inadequate for 40 kTPI, so the latest drives incorporate an eccentricity compensation function. The AL series devices apply a very strong compensation for eccentricity, which is measured using a DFT in the frequency domain, and use a hybrid combination of feedforward and feedback control. As shown in Figure 6, the 1st to 6th harmonics are eliminated completely and we can select higher order harmonics, for example, the 12<sup>th</sup> and 18<sup>th</sup>. However, for the compensation of higher order harmonics, we have to consider the phase relations of RRO between the different cylinders. If the cylinders are out of phase, the compensation sometimes increases the RRO.

#### 4.5 Disturbance suppression control

If we get a higher servo gain, the TPI can be



Figure 14  
MFM photograph of position signal on AL-7LE media.

increased even higher. Therefore, increasing the disturbance durability is an important goal for good system reliability. The most severe disturbance is a mechanical interaction between the drives that is often seen in low-stiffness RAID cabinets.<sup>16)</sup> To suppress such a mechanical interaction, stiffer cabinets are recommended.

To minimize the influence of mechanical interaction, the open-loop transfer function was optimized. We apply a rugged disturbance tuning using a special combination of feedback and feedforward control. The effect of this method is nearly equivalent to setting a higher integrator gain. Because the cabinet resonance is at several hundreds of Hz, the loop gain must be increased to over several hundreds of Hz to suppress the interaction effect. In generic use, this servo system provides adequate performance. However, for a special low-stiffness cabinet, this method is not enough. To suppress the interaction further, acceleration feedforward control using dual piezoelectric accelerometers is very effective.<sup>17)</sup> This is the most robust method for very strong disturbances (**Figure 15**). If the current trend of TPI-increase continues, this control will be indispensable for server drives.

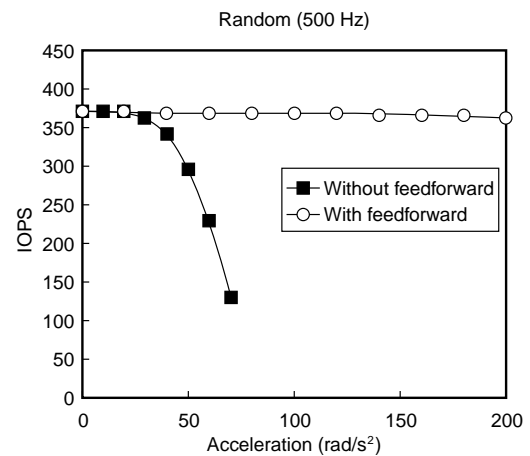


Figure 15  
Rotational vibration durability with and without feedforward.

## 5. Making the 10/15 krpm drives quiet

Increasing the rotational speed to as high as 15 krpm and the seek acceleration to as high as 220 G will generally increase the power consumption and acoustic noise. PC servers are usually installed in ordinary office spaces (unlike large-scale servers) and use many drives in a RAID system. Therefore, it is important for customers that the drives be quiet. Our target is to build drives that are quiet enough to use in a home at midnight. Our final target is in the region of 3.0 Bels of sound power. **Table 2** shows the measured acoustic noise for the AL drives. These noise levels are some of the lowest for currently available high-rpm SCSI drives.

To achieve a lower sound power, we started by measuring the acceleration at the top cover and base casting, because generally, there is a strong correlation between acceleration and sound pressure. Then, based on the measurements, we adjusted the resonance of the spindle motor switching to reduce the sound level. Generally, the mass of the top cover is important here. We also reduced the sound level by damping resonance and by using insulation sheets between the base casting and the printed circuit board. Insulating the top cover also had a big effect.

Accelerating components at 220 G for several milliseconds is like hitting them with a hammer. Some ATA drives have a "silent seeking" mode with slower seeking. If we double the seek time, the sound power decreases dramatically. Howev-

er, in the case of server applications, we cannot afford to slow down the seek time. The seek tone depends on the seek waveform and the mechanical transfer function. The strongest noise source is the fundamental actuator resonance, and the higher resonances generate less noise. Furthermore, a rigid mechanism tends to radiate pleasant tones. The AL-7LE/LX seek tones are probably acceptable by most people.

In addition, we must point out the seek noise in consumer PC cabinets. Because the 3.5-inch bay in a PC case is typically made of thin metal, the bay amplifies the seek noise. The most effective countermeasure is to add a heavier damping sheet with a metal and adhesive layer to the bay. A damping sheet made of lead will dramatically improve the seek acoustics.

Because of their high rotational speed, the AL 10 krpm and 15 krpm drives apply strict dual plane balancing to reduce spindle rotational vibration. Since the centrifugal force in 15 krpm drives is 2.25 times larger than in 10 krpm drives, we decided that the residual spindle imbalance must be half of the value in the 10 krpm drives. As a result, you cannot feel any rotational vibration when you touch an operating 15 krpm drive.

## 6. Reliability

Fujitsu's drives have a top level of reliability, and this has been confirmed many times by our customers. Next, we will look at some issues of reliability.

### 6.1 Bearing reliability

We do not have enough drives in the field that run at 15 krpm to learn enough about their long-term reliability. Therefore, we conducted continuous accelerated life tests on these drives. The lifetime is governed by the bearing life. Since the general acceleration ratio is doubled every 10°C, based on 6000 hours of testing at 80°C, we can assure a lifetime of 50 000 hours, or 5.7 years of continuous use, at 50°C.

**Figure 16** shows the sound pressure and

Table 2  
Measured acoustic noise.

		Sound power (Bels)	
		Ready	Seek
AL-7LE	73 GB	3.70	4.16
	36 GB	3.36	3.77
	18 GB	3.32	3.77
AL-7LX	36 GB	3.69	4.03
	18 GB	3.48	3.95

These are average values for 5 drives.

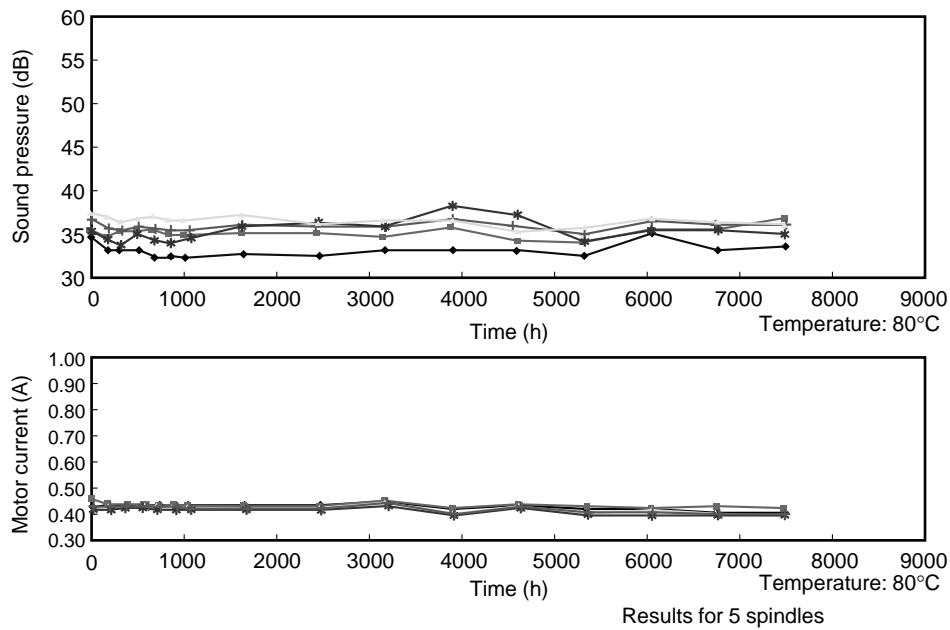


Figure 16  
Accelerated life test of 15 krpm spindle.

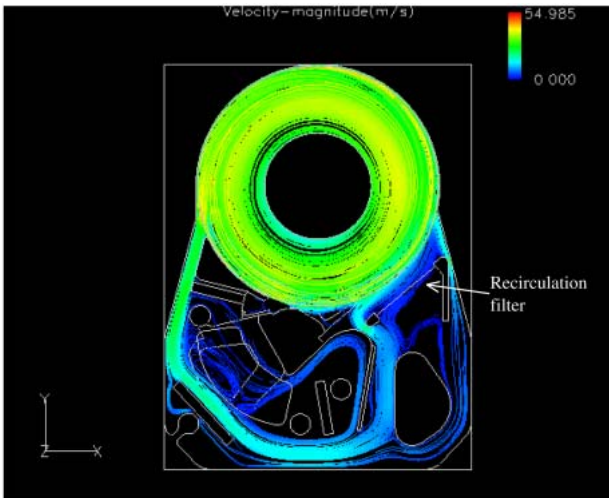


Figure 17  
Streamline plot in AL-7LX (15 krpm).

motor driving current of drives with ceramic ball bearings running at 15 krpm during an accelerated life test at 80°C. In the case of ball bearings, measuring the sound pressure is the most sensitive evaluation method, because a drive’s sound usually degrades before there is any observable reduction in rotational accuracy. We cannot see any sign of degradation of acoustic noise or motor

driving current in the figure, and therefore conclude that the ceramic bearings can withstand more than 6000 hours in the accelerated life test without degrading. Furthermore, a new type of Ferro-fluidic seal which has a longer life in all temperature ranges was used in the ceramic bearing spindle. Figure 16 also shows, therefore, that the new Ferro-fluidic seal has a sufficiently long life.

For the 10 krpm drives, we use field-proven steel ball bearings. We apply the CSS technology (non load/unload); therefore, there is no risk of “fretting injury” during transportation.

## 6.2 Contamination control

The level of cleanliness in all of our drives is of course extremely high, but the new drives’ flying height of only 14 nm requires an even higher level. **Figure 17** shows a simulation of the filtration in the drive. The flow around the recirculation filter is smooth, and there is no stagnation area. The effectiveness of filtration is defined in terms of the particle decade decay time. This indicates the necessary number of seconds for the number of particles to fall by a factor of 10. The measured

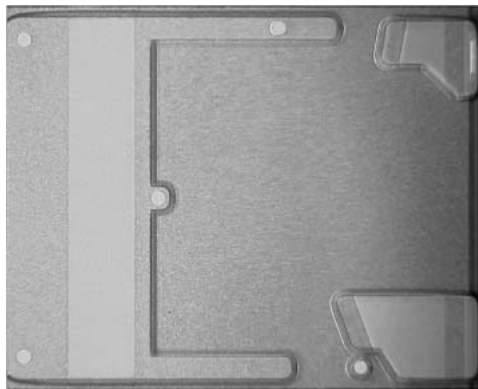


Figure 18  
Air bearing surface of advanced stiction free slider.

decade decay time in our 15 krpm drives was around 6 seconds. The calculated decay time using the simulated flow rate at the recirculation filter shown in Figure 17 agrees fairly well with the measured decay time. The calculation method is described in Reference 18).

Judging from the results of the flow simulation, we estimate that contamination is well controlled in these drives.

### 6.3 Stiction free (SF) slider technology<sup>19)</sup>

Without using the load/unload method, Fujitsu has developed a unique stiction free (SF) slider which has small pads on the air bearing surface (Figure 18). Because the pads are made of thin diamond-like carbon (DLC), they have excellent resistance to abrasion and adhesion when the lubricant thickness and drive humidity are strictly controlled. Thanks to the SF technology, we do not see any adhesion problems in the drive.

## 7. Benchmark performance

Lastly, we evaluate our AL drives using the results of benchmark tests we conducted on a desktop PC. We tested the 36 GB AL-7LE (10 krpm), the 36 GB AL-7LX (15 krpm), and a typical 60 GB 7200 rpm ATA drive for comparison. The benchmark test results are shown in Figure 19.

In the sequential read test (64 k-byte blocks),

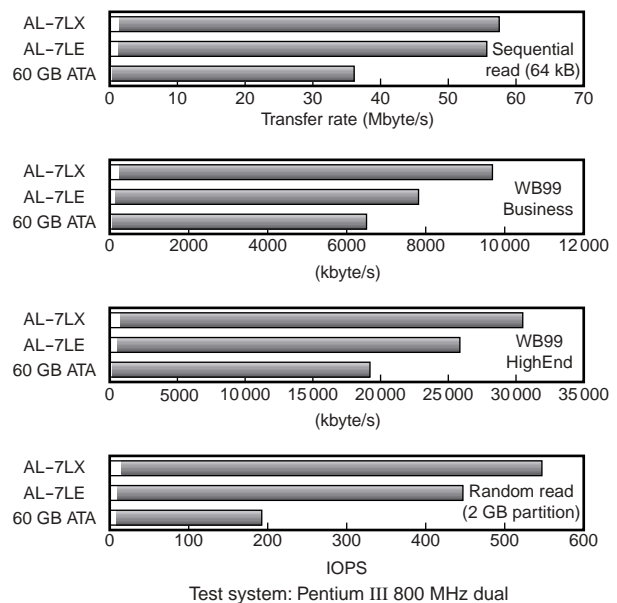


Figure 19  
AL-7s benchmark results.

the LE and LX drives transferred data at more than 56 Mbyte/s. However, between the LE and LX, the sustain transfer rate did not differ in proportion to the media transfer rate difference. This is because the higher rpm drives have a higher head/cylinder skew-time ratio. The LX was more than 20% faster than the LE in every test except the sequential read test. Especially, in the WinBench99 High End test, the LX demonstrated a transfer rate of more than 30 Mbyte/s, which is more than 50% faster than the rate achieved by the 7200 rpm ATA drive.

In the random test, the LE and LX drives were 2.5 to 3 times faster than the ATA drive. The difference between the LE and LX is mainly caused by their different seek times.

We can conclude that AL-7LE/LX high-rpm SCSI drives have a much better performance than the 7200 rpm ATA drive and that the 15 krpm LX has the best performance among the three. These results show that the AL-7LE/LX SCSI drives are the best choice for both enterprise and desktop PC applications.

## 8. Conclusion

This paper described the mechanical performance of Fujitsu's new AL-7 series of 10/15 krpm SCSI hard disk drives. To achieve a high track density of 40 kTPI at 10/15 krpm, it was necessary to reduce the drives' NRRO. We therefore stabilized the airflow using the results of aerodynamic simulation and then reduced the resonance of the motor spindle, which is another cause of NRRO. As a result, we were able to reduce the six-sigma NRRO to less than 85 nm.

This paper then described how we achieved the fast access time needed for the high TPIs of these drives by employing a newly developed rigid, lightweight actuator. The high 1.4 kHz servo-mechanism bandwidth of this actuator enables a fast average seek time of 3.5 ms at 40 kTPI.

We then described how we reduced the acoustic noise of these high-rpm drives and explained that an accelerated life test indicated that the 15 krpm drives could be operated with ceramic ball bearings for at least 50 000 hours. Then, we discussed the subject of contamination control and described our stiction free slider technology.

Finally, we presented the results of benchmark tests we conducted indicating that the performance of these 10/15 krpm SCSI drives makes them suitable for enterprise applications.

Fujitsu's AL-7 series of high-performance hard disk drives complement today's high-speed processors and are appropriate not only for servers but also for desktop PCs.

We will continue to develop drives with even higher performance figures to meet our customers' needs.

## Acknowledgement

We would like to thank the engineers of the design team, manufacturing team, evaluation/qualification team, and customer support team for making these advanced drives a reality. Also, we would like to thank the many industrious and enthusiastic customers who have helped the developers create the AL series. The existence of

the AL series is completely due to the excellent collaboration between these customers and Fujitsu.

## References

- 1) M. Fujino, J. Sugihara, and S. Ogawa: Magnetic disk storage. *FUJITSU Sci. Tech. J.*, **21**, 4, p.395-407 (1985).
- 2) Y. Mizoshita: New technologies for Hard Disk Drives. (in Japanese), *FUJITSU*, **50**, 1, p.14-21 (1999).
- 3) M. Sekino: High-performance Hard Disk Drives for servers. (in Japanese), *FUJITSU*, **50**, 1, p.22-27 (1999).
- 4) H. Kanai, K. Noma, and J. Hong: Advanced Spin-Valve GMR Head. *FUJITSU Sci. Tech. J.*, **37**, 2, p.174-182 (2001).
- 5) E. N. Abarra, B. R. Acharya, A. Inomata, A. Ajan, and I. Okamoto: Synthetic Ferrimagnetic Media. *FUJITSU Sci. Tech. J.*, **37**, 2, p.145-154 (2001).
- 6) S. Deeyiengyang and K. Ono: Suppression of resonance amplitude of disk vibrations by squeeze air bearing plate. *IEEE Trans. Magn.*, **37**, 2, p.820-825 (2001).
- 7) S. Imai: Fluid dynamics mechanism of disk flutter by measuring the pressure between disks. *IEEE Trans. Magn.*, **37**, 2, p.837-841 (2001).
- 8) M. Tatewaki, N. Tsuda, and T. Maruyama: An analysis of disk flutter in hard disk drives in aerodynamic simulation. *IEEE Trans. Magn.*, **37**, 2, p.842-846 (2001).
- 9) H. Shimizu, M. Tokuyama, S. Imai, S. Nakamura, and K. Sakai: Study of aerodynamic characteristics in Hard Disk Drives by numerical simulation. *IEEE Trans. Magn.*, **37**, 2, p.831-836 (2001).
- 10) H. Kubotera, N. Tsuda, M. Tatewaki, S. Noda, M. Hashiguchi, and T. Maruyama: Computational fluid analysis of internal air flow in Hard Disk Drives. (in Japanese), *Proc. JASME*, **IV**, 01-1, p.235-236 (2001).
- 11) H. Kubotera, N. Tsuda, M. Tatewaki, and T.

- Maruyama: Aerodynamic vibration mechanism of HDD arms predicted by unsteady numerical simulations. *Intermag 2002*, (to be published).
- 12) I. Y. Shen and C. P. Roger Ku: A nonclassical vibration analysis of multiple rotating disk/spindle system. *ASME I. Appl. Mech.*, **64**, p.165-174 (1997).
  - 13) A. Hartman: Undriven vibrations in brushless DC motors. *IEEE Trans. Magn.*, **37**, 2, p.789-792 (2001).
  - 14) Y. Uematsu, M. Fukushi, and K. Taniguchi: Development of the pushpin-free STW. *IEEE Trans. Magn.*, **37**, 2, p.964-968 (2001).
  - 15) T. Asada, H. Saitou, Y. Asaida, and K. Itoh: Characteristic analysis of hydrodynamic bearings for HDDs. *IEEE Trans. Mag.*, **37**, 2, p.810-814 (2001).
  - 16) M. Suwa and K. Aruga: Evaluation system for residual vibration from HDD mounting mechanisms. *IEEE Trans. Magn.*, **35**, 2, p.868-873 (1999).
  - 17) A. Jinzenji, T. Sasamoto, K. Aikawa, S. Yoshida, and K. Aruga: Acceleration feedforward control against rotational disturbance in Hard Disk Drives. *IEEE Trans. Mag.*, **37**, 2, p.888-893 (2001).
  - 18) K. Aruga, Y. Mizhoshita, and M. Sekino: Structural design for high-performance magnetic disk drives. *FUJITSU Sci. Tech. J.*, **26**, 4, p.365-377 (1991).
  - 19) T. Yamamoto, T. Yokohata, and Y. Kasamatsu: Stiction Free Slider for a lightly textured disk. *IEEE Trans. Magn.*, **34**, p.1783-1785 (1998).



**Keiji Aruga** received the B.S. and M.S. degrees in Mechanical Engineering from the University of Tokyo in 1975 and 1977, respectively. He joined Fujitsu Ltd. in 1977, where he has been engaged in development of hard disk drives. He is the chief of the mechanical design team for the AL-4 to AL-7 drives. He is a member of the Japan Society of Mechanical Engineers (JSME).

E-mail: aruga@jp.fujitsu.com